MULTIVARIABLE AIRCRAFT CONTROL BY MANOEUVRE COMMANDS – AN APPLICATION TO AIR-TO-GROUND GUNNERY

Dang Vu Binh

Office National d'Etudes et de Recherches Aérospatiales (ONERA)
92320 Châtillon (France)

Abstract

This paper describes a concept of aircraft control in which the pilot commands are variables directly related to the aircraft motion in opposition to deflexion angles of control surfaces. It is the airborne computer which synthesizes and coordinates the commands for the various control surfaces, so that the aircraft reaches the manoeuvre goal set by the pilot.

Two examples of manoeuvre commands have been considered :

– the first example corresponds to a common mode of aircraft control whereby the pilot sets the sideslip, roll rate and pitch rate ; the control law is briefly described and then evaluated by digital simulation in the final phase of an air-to-ground gunfiring ;

– the second example is specific to the air-to-ground gunnery ; an approach to designing an Integrated Flight and Fire Control (IFFC) system is presented whereby the pilot's task is reduced to target designation.

The design of both control systems is based on linear optimal control theory with model-following improvement.

Nomenclature

α	angle of attack
β	sideslip angle
p, q, r	body-axis roll, pitch, yaw angular rates
v, w	aircraft speed components in the body -Y and Z axes
ϕ, θ	roll, pitch Euler angles
δ_ℓ	aileron surface deflexion
δ_m	elevator deflexion
δ_n	rudder deflexion
δ_{dsf}	direct side force surface deflexion
Σ_v, Σ_w	gun aiming errors
R	range from aircraft to target
h_y, h_z	bullet ballistic corrections
u	command vector
x	state vector
V	aircraft speed relative to the surrounding air
v_w, w_w	wind components in the body -Y and Z axes
V_K	aircraft speed relative to the Earth
τ	aircraft remaining time of flight to target

Superscript

*	desired values

I. Introduction

Improved handling qualities of aircraft are one of the most sought after goals in the use of fly-by-wire control systems. These systems provide aircraft stability, optimization of flight configuration and navigation, decreased aircraft sensitivity to turbulence.

In this Control Configured Vehicle (CCV) concept, multivariable aircraft control by manoeuvre commands or task-oriented control[1] is a control strategy whereby the pilot has the possibility to command at will individual state variables of the aircraft motion, or combination of these state variables, instead of control surface deflexions. Usually, the realization of a manoeuvre command necessitates an acute coordination of many control surface deflexions, and the result is strongly dependent on the pilot's skill. With this emerging concept of control, the pilot can command directly the desired effect (e.g. roll rate, pitch rate, sideslip, pitch attitude), leaving to the control system the task of optimization and coordination of the appropriate control surfaces, so that the objective set by the pilot is accurately achieved.

This concept of aircraft control can reduce considerably the pilot's workload during critical flight phases such as the final phase of air-to-ground gunfiring, where precision flying is especially required. There is indeed a continuing need to increase the weapon accuracy of gunnery which is brought by the fact that it is unattractive to expend high-cost guided weapons to destroy low-cost targets. Sophisticated weapon-aiming systems have been developed to assist the pilot in the task of aiming, but the destruction of the target still depends on the pilot's skill to control the aircraft. For example, the sideslip control is normally the result of a coordinated action of the pilot on both aileron and rudder ; this can be done automatically in the task-oriented control concept.

In Section II, a mathematical model of the aircraft dynamics, kinematics of a typical air-to-ground gunnery pass involving computation of bullet impact point are expressed in state variable form which is well-suited for the application of modern optimal control techniques.

Section III summarizes the control law design of a command system whereby the pilot inputs are chosen to be the roll rate, pitch rate and sideslip [2]. The command system has been tested to null aiming errors during the final phase of an air-to-ground gunnery pass.

The very short duration of the pass (about 10 seconds) justifies consideration of another kind of control more specifically adaptable to this flight phase ; this control is accomplished by the coupling of the fire and the flight control systems. The pilot action is limited to the sole designation of the target and aiming errors are nulled automatically. Section IV presents an approach for

designing such a system, called Integrated Flight and Fire Control (IFFC) system [3], which provides an expanded gunnery envelope and improved accuracy.

II. Model of the aircraft dynamics and air-to-ground gunnery kinematics

II.1. Aircraft dynamics and description of the gunnery pass

In this paper we consider only the final phase of air-to-ground gunfiring. Since the duration of the pass is relatively short, say about 10 seconds, it is appropriate to assume the aircraft velocity to be constant. Because of this assumption the dynamic force equation along the longitudinal aircraft X-axis may be neglected and then the non-linear dynamic and kinematic equations of the aircraft model can be expressed by the following 7th order differential equation, see Appendix 1 :

$$\dot{x} = f(x, u, V_w) \qquad (1)$$

where

$$x^T = (v, w, p, q, r, \Phi, \theta) \qquad (2)$$

is the state vector (see nomenclature for the meaning of the different components), and

$$u^T = (\delta_l, \delta_m, \delta_n, \delta_{DSF}) \qquad (3)$$

is the control vector including moment control surfaces (aileron δ_l , elevator δ_m , rudder δ_n) as well as direct force control surfaces (direct side force δ_{DSF} only). The principal disturbance input V_w will be a steady lateral wind, which is of primary interest in the air-to-ground gunnery.

The gunnery pass, depicted in Fig. 1, is a low altitude attack where firing range is typically short (under 2,000 m) and gun pointing precision especially required with the use of 30-mm cannon. The ground attack simulation runs start from 2,500 m-range to target and 500 m-altitude in a 10 degree dive, and stop at the beginning of the evasive manoeuvre when range to target reaches 500 metres. Aircraft speed is fixed at 230 m/s (M = 0.68) and target velocity has been assumed zero for simplifying.

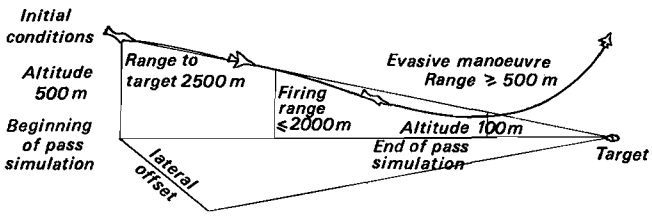

Fig. 1 — Typical gunnery attack profile.

II.2. Computation of the bullet impact point

The basic air-to-ground gunnery mode of weapon-aiming systems is CCIP (Continuously Computed Impact Point) (see Fig. 2). The ballistic trajectory of the bullet is dependent on the aircraft velocity vector and on any other additional velocity or acceleration imparted upon the projectile itself. Since aircraft control laws are of primary interest here, the problem of determining the impact point will be simplified by using the following expressions for its angular coordinates in the aircraft reference frame[4]:

$$h_y = C_\beta + C_g \sin\Phi \qquad (4)$$

$$h_z = C_\alpha + C_g \cos\Phi + \theta_g + C_{px} \ , \qquad (5)$$

where

$C_\beta = \frac{V_K}{V_K+V_m}(\beta+\beta_w)$: aim error introduced by gun sideslip

$C_\alpha = \frac{V_K}{V_K+V_m}(\alpha-\theta_g)$: aim error introduced by gun angle of attack

V_m : bullet muzzle velocity (V_m = 815 m/s for the 30-mm ammunition)

β_w : sideslip angle due to crosswind

θ_g : gun depression below aircraft X-axis

C_{px} : parallax correction for head-up-display (HUD).

C_g is the gravity drop and can be approximated by the following expression, resulting from theoretical and experimental studies [4] :

$$C_g = \frac{1}{2} g \frac{R}{\sqrt{V_K+V_m}\, U^{3/2}} \cos(C_\alpha + \theta_g - \theta) \ ,$$

where R is the slant range from the aircraft to the target, and

$$U = V_K + V_m - k R \sqrt{V_K+V_m}$$

is the mean velocity of the bullet along the range R. k is a characteristic coefficient of the bullet (k = 0.01 $m^{-1/2}$ $s^{-1/2}$ for the 30-mm ammunition).

V_K , α , β , Φ and θ are related to the state vector of the aircraft (see nomenclature).

Expressions (4) and (5) show that the ballistic corrections are only dependent on the state vector x and

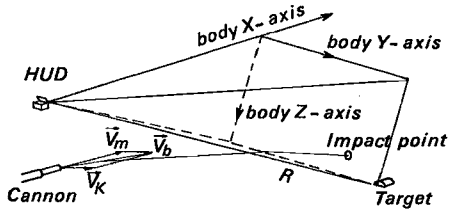

Fig. 2 — Air-to-ground gunnery display.

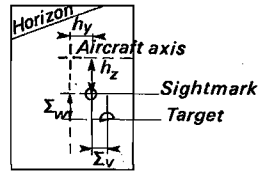

$\vec{V}_b = \vec{V}_K + \vec{V}_m$ = *initial velocity of bullet*

the slant range R. The impact point of the bullet is displayed on the HUD ; when the sightmark crosses the target, the pilot releases his weapon (see Fig. 2).

II.3. Aiming errors kinematic

The aiming errors are given by

$$\Sigma_v = \frac{Y}{R} - h_y \qquad (6)$$

$$\Sigma_w = \frac{Z}{R} - h_z \quad , \qquad (7)$$

where Y, Z are the coordinates of the target in the aircraft reference frame. Expressing $\dot{Y}$, $\dot{Z}$ leads to the following differential equations that define the aiming errors kinematic :

$$\dot{\Sigma}_v = -\frac{v}{V\tau} - r + \frac{\Sigma_v}{\tau} + \eta_v \qquad (8)$$

$$\dot{\Sigma}_w = -\frac{w}{V\tau} + q + \frac{\Sigma_w}{\tau} + \eta_w \quad , \qquad (9)$$

where

$$\tau = \frac{R}{V} = \frac{R_0}{V} - t \qquad (10)$$

is the aircraft remaining time of flight to target, and η_v and η_w are related at first order to ballistic corrections and crosswind :

$$\eta_v = -\frac{v_w}{V\tau} + \left(\frac{h_y}{\tau} - \dot{h}_y\right) + p\,(\Sigma_w + h_z) \qquad (11)$$

$$\eta_w = -\frac{w_w}{V\tau} + \left(\frac{h_z}{\tau} - \dot{h}_z\right) - p\,(\Sigma_v + h_y) \quad . \qquad (12)$$

Examination of (8) and (9) reveals the fundamental instability of the kinematics.

Defining the vector aiming error

$$y^T = (\Sigma_v, \Sigma_w) \quad , \qquad (13)$$

equations (8) and (9) can be combined into a state variable model of aim error of the form

$$\dot{y} = g(x, y, \tau, V_w) \quad . \qquad (14)$$

Thus, equations (1) and (14) describe the whole model adopted for the aircraft dynamics and the gunnery kinematics.

III. Sideslip, roll rate and pitch rate control

III.1. Description of the controller

A two-level flight control system for nonlinear aircraft motion has been designed [2] which realizes a task-oriented control and an augmentation of the aircraft stability within a wide manoeuvring envelope.

A nonlinear model of the aircraft dynamics, incorporating inertial coupling terms and nonlinear aerodynamic effect is used to define the first level of control (see Fig.3). At this level are computed reference state x_m and actuator control trajectories u_m and an output vector z_m which pursues the manoeuvre command z_d set by the pilot with specified dynamics ; the pilot inputs comprise the sideslip β (or $v = \beta V$, component of the aircraft velocity vector V along the body Y-axis), the roll rate and the pitch rate.

At a second level, a servocompensator controls the aircraft to follow the motions of the model. The control law is obtained by application of optimal control theory to locally linearized aircraft dynamic equations, corresponding to quasi-steady flight conditions.

Figure 3 presents the control system in block-diagram form.

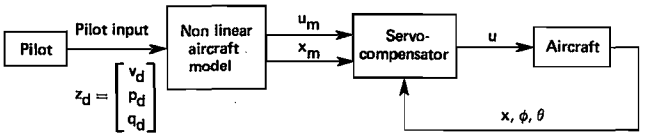

Fig. 3 –Block diagram of (v, p, q) control system.

Here, the reduced state vector is defined as

$$x^T = (v, w, p, q, r) \quad ,$$

and the kinematic state variables (Φ , θ) are treated as uncontrolled variables for the reduced-order system. Direct side force is not available so that the control vector is defined as

$$u^T = (\delta_\ell , \delta_m , \delta_n) \quad .$$

The components of the manoeuvre command vector are

$$z^T = (v, p, q) \quad .$$

In order to obtain smooth acceleration responses to wind gusts, the vector

$$\tilde{x}^T = (a_y, a_z , p, q , r)$$

has been introduced, where

a_y is the lateral acceleration

a_z is the normal acceleration.

The control law is given by the following expression[2]:

$$u = u_m + K_p\,(\tilde{x} - \tilde{x}_m) + K_I \int_0^t (z - z_m)\,ds \quad . \qquad (15)$$

The feedback regulator is a proportional-integral controller ; discrepancies between aircraft and model motions are continuously corrected by the proportional term ; zero steady-state error is realized by the integral term. The nonlinear aspect of the aircraft model allows the use of this control system in a wide manoeuvring envelope, especially when command inputs are roll rates of large magnitude.

III.2. Typical manoeuvre commands for nulling aiming errors

The control system described above is adaptable for a general mode of aircraft control. However, it has been evaluated in the task of nulling aiming errors during an air-to-ground gunnery pass with fixed depressed reticle sight set for a 500 metre-firing range ($h_y = 0$ and $h_z = 1.4°$) The pilot inputs are supposed to be a fast succession of step inputs in roll rate and pitch rate. Sideslip command is set to zero. Aircraft motions and aiming error responses to initial longitudinal and lateral offsets are shown in

Figures 4 and 5. Aircraft data and feedback gains used in the numerical example are given in Appendix 2.

It is appropriate to note that Figures 4 and 5 present aiming error responses only to elementary inputs. For a real pass, the pilot closes the loop by changing continuously the roll rate and pitch rate commands. Yet, the displayed results indicate that longitudinal offset can be easily nulled through pitch rate command but that lateral aiming error has a longer time of response. Indeed, examination of Eq. (8) shows that yaw rate command should be preferred to roll rate command to null lateral offset. Anyway, faster response in lateral aiming would be achieved with the (v, p, q) control system if the specified dynamics (in particular the time of response of roll rate) of the aircraft model at the first level of the controller were improved with respect to the numerical example presented in Figure 5.

It would be of great interest to see how a control system based on pitch rate, yaw rate, and eventually sideslip commands would behave in similar air-to-ground gunnery simulations. Implementation has been made using other controller designs[5] ; it is in progress for this particular kind of model-following regulator.

In the next section, another realization is described for the aircraft controller which presents advantages of a different nature, and is especially attractive for the air-to-ground gunnery.

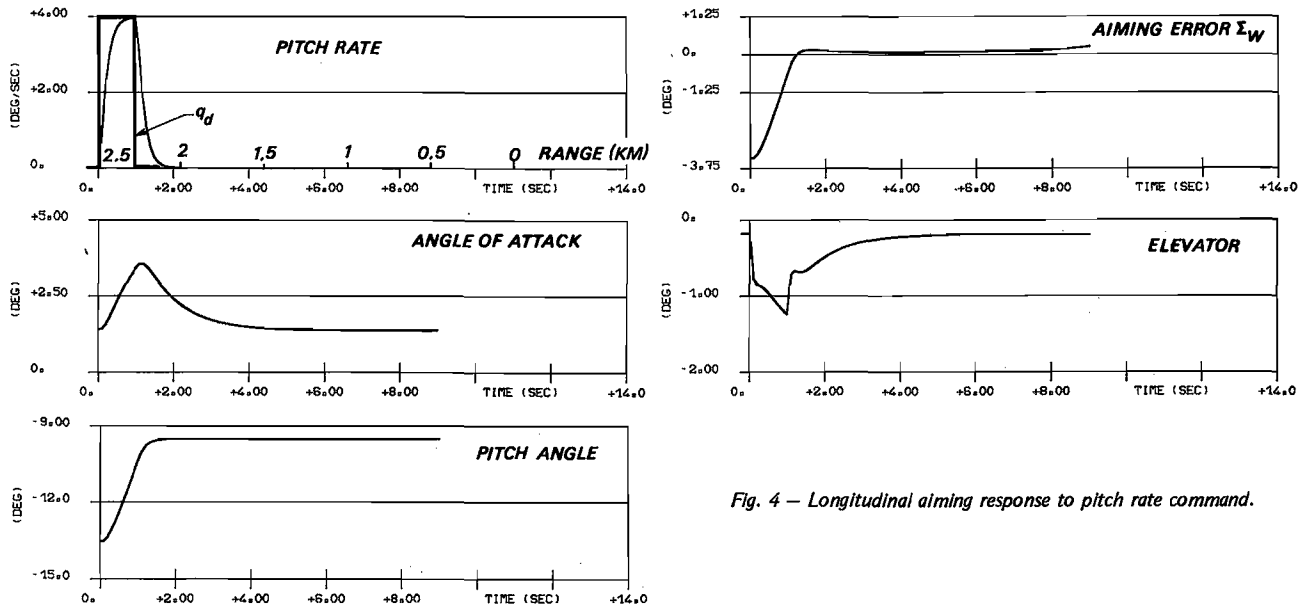

Fig. 4 — Longitudinal aiming response to pitch rate command.

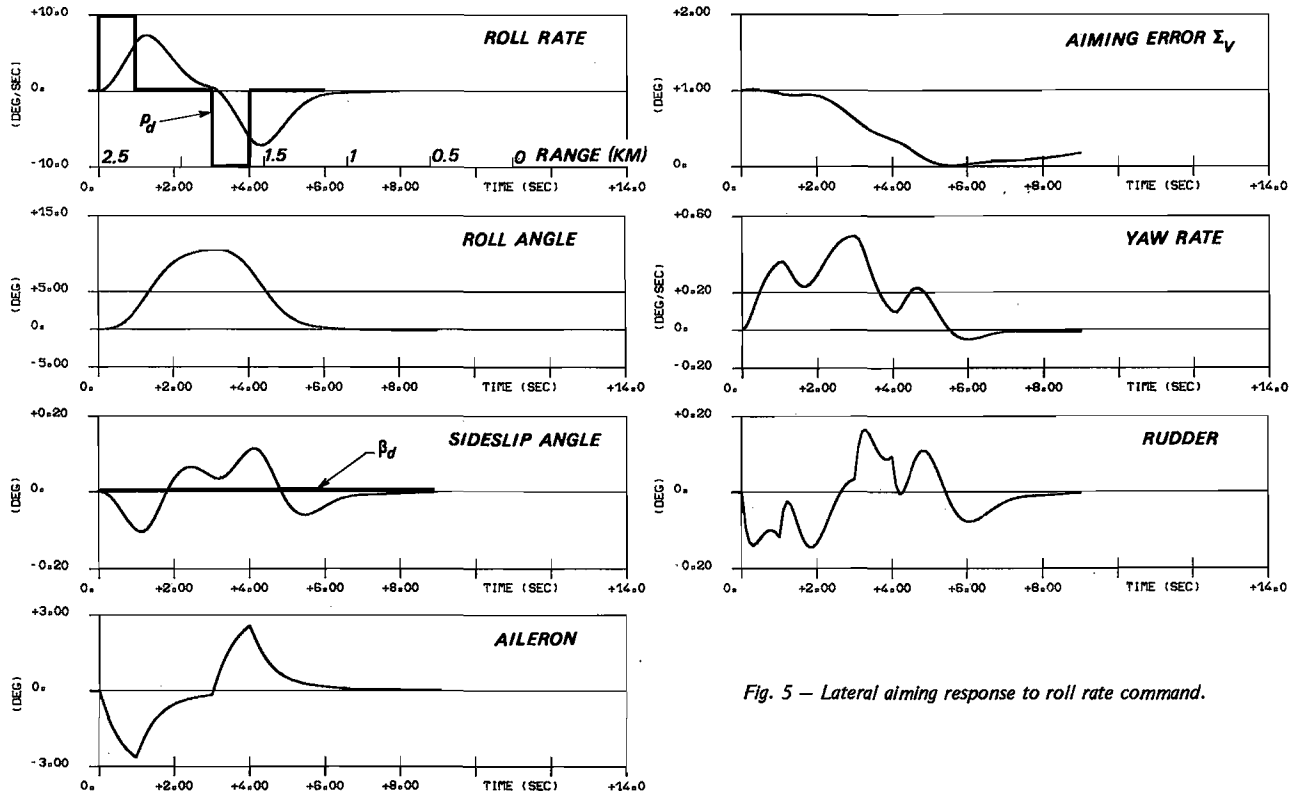

Fig. 5 — Lateral aiming response to roll rate command.

IV. Aim error control

Large improvements have been achieved using the controller described in Section III with respect to conventional (manual) aircraft control. However, it appears that during the gunnery pass, the pilot has only a short time interval to line up the sightmark on the target. In order to reduce further the pilot's workload, a new concept combining flight and fire controls into a single automatic control is proposed. The approach taken here is to consider aiming errors as state variables to be retained in the design of the control system. An important improvement is that automatic coordination between pitch rate, roll rate, yaw rate and other commands is achieved while the only inputs provided by the pilot are angular errors as seen in the HUD.

IV.1. Development of the control law

Linearization : The nonlinear dynamic and kinematic equations (1) and (14) have been linearized in the usual way with respect to a reference flight condition. Often, rectilinear flight or quasi-steady flight has been chosen for this reference trajectory. Linearization of Eq (14) for a rectilinear flight path leads to the presence of a forcing term in the resulting equation ; this term is due to the variation of bullet ballistic corrections with range. Such a linear problem with forcing term can be solved [6] but this is complicated. Then, it is more appropriate to adopt a reference aircraft trajectory along which bullet ballistic corrections are taken into account such that aiming errors are continuously nulled. In other words, the desired flight path corresponds to a continuous alignment of the sightmark with the target. Using the notations of Section II, we have

$$y^* = 0 \tag{16}$$

and

$$\dot{y}^* = 0 \ , \tag{17}$$

where the superscript symbol (*) denotes the desired value of a variable.

The desired flight path can be described by specifying the values of the state vector x corresponding to this flight condition. Thus, assuming that $x^*(t)$ describes the desired flight path, then the error in the actual flight path is

$$\Delta x(t) = x(t) - x^*(t) \tag{18}$$

$$\Delta y(t) = y(t) - y^*(t) = y(t) \ . \tag{19}$$

Expanding the dynamic and kinematic equations (1) and (14) in first-order Taylor series leads to the following linear time-varying system involving the perturbation vectors :

$$\Delta\dot{x} = A\,\Delta x + B\,\Delta u \tag{20}$$

$$\dot{y} = C(t)\Delta x + D(t)y + E\,\Delta u \ . \tag{21}$$

A and B are the partial derivative matrices of the vector function f with respect to x, u and V_w ; C, D and E are the partial derivative matrices of the vector function g with respect to x, y, u and V_w. Note that the perturbation on component V_w can be expressed into a perturbation on the state vector x since V_w is assumed to be a steady crosswind.

The matrices C and D depend on time through the parameter τ which is the aircraft remaining flight time to target.

The nominal vectors satisfy the following equations,

$$\dot{x}^* = f(x^*, u^*, V_w) \tag{22}$$

$$0 = g(x^*, 0, \tau, V_w) \tag{23}$$

where x^*, and u^* are defined by (2) and (3).

Control law : Since the objective is to follow the desired flight path, x^*, it is appropriate to minimize a cost function which is quadratic in the error Δx. Furthermore, one would like the system given by Eq. (21) to behave as closely as possible as the following differential system,

$$\dot{y}_m = A_m y_m \tag{24}$$

that represents the model of desirable aim error kinematics.

In implicit model-following, the above objective is realized by using a control law that minimizes a performance index of the form [7]

$$J = \int_{t_o}^{t_f} [\Delta x^T Q_1 \Delta x + (\dot{y} - A_m y)^T Q_2 (\dot{y} - A_m y) + \Delta u^T R_1 \Delta u]\,dt + \Delta x^T(t_f) S_1 \Delta x(t_f) + (\dot{y} - A_m y)^T(t_f) S_2 (\dot{y} - A_m y)(t_f) \ , \tag{25}$$

where t_o and t_f are the times corresponding to the beginning and end of the pass. By substituting (21) for $\dot{y}$ in (25), and defining an augmented state X as :

$$\Delta\dot{X} = \begin{bmatrix}\Delta\dot{x}\\ \dot{y}\end{bmatrix} = \begin{bmatrix}A & 0\\ C & D\end{bmatrix}\begin{bmatrix}\Delta x\\ y\end{bmatrix} + \begin{bmatrix}B\\ E\end{bmatrix}\Delta u \ , \tag{26}$$

the cost function reduces to a more usual form

$$J = \int_{t_o}^{t_f} (\Delta X^T Q \Delta X + 2\Delta X^T M \Delta u + \Delta u^T R \Delta u)\,dt + \Delta X^T(t_f) S \Delta X(t_f) + 2\,\Delta X^T(t_f) N \Delta u(t_f) \ . \tag{27}$$

As it is well known, minimization of (27) results in a linear control law [8]

$$\Delta u = K \Delta X \ , \tag{28}$$

or

$$u(t) = u^*(t) + K_1(t)[x(t) - x^*(t)] + K_2(t) y(t) \ . \tag{29}$$

x^* and u^* are derived from the computation of the desired flight path. The optimal gain matrix $K = [K_1 \ K_2]$ depends on time only through the parameter τ or range to target.

It is assumed that all state variables, included aiming error vector, are available for feedback.

Desired flight path : The desired path is defined by Eqs. (22) and (23). The 9th order nonlinear system in 11 unknowns (i.e. x^* and u^*) has generally an infinity of solutions. One way to address the problem is to increase the order of the system by using two constraints involving roll angle and sideslip :

$$\phi^* = 0 \qquad (30)$$

$$v^* = 0 \ . \qquad (31)$$

Only one constraint is required to complete the system if direct side force is not available. Thus, additional Eq. (30) has been retained to solve the problem of determining the desired flight path in this case.

The desired longitudinal motion is characterized by a slight and continuous dive along a curved flight path where pitch rate and angle of attack are related by the following expression derived from Eq. (9),

$$\frac{\alpha^*}{\tau} - q^* = \frac{h_z^*}{\tau} - \dot{h}_z^* \qquad (32)$$

It can be shown that the desired value of pitch rate decreases with range as bullet ballistic corrections become less important.

Desired lateral motion under a steady crosswind : In presence of crosswind, the first constraint $\phi^* = 0$ may be kept to solve the problem since it is well known that direct side force (DSF) can be used to trim out crosswind while maintaining a wings-level attitude. For the desired value of sideslip, two weapon delivery configurations have been considered (see Fig. 6), leading to two kinds of control law :

– weapon delivery with aircraft sideslip (decrab mode)

$$v^* = -v_w \qquad (33)$$

– weapon delivery without aircraft sideslip (crab mode)

$$v^* = 0 \ . \qquad (34)$$

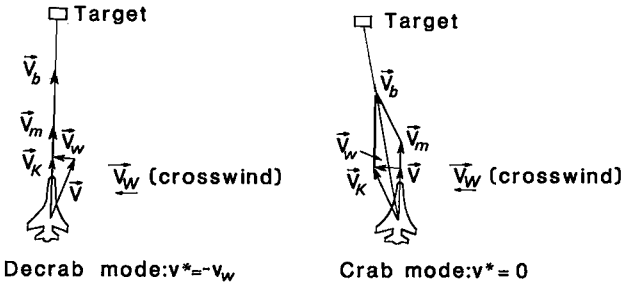

Fig. 6 – The two weapon delivery configurations.

The decrab mode is designed to maintain the aircraft trajectory in a vertical plane containing the target thus achieving zero crab angle. Substituting Eq (30) and Eq (33) in Eqs (4) (8) (11) leads indeed to the following desired values for yaw rate and roll rate,

$$r^* = 0 \qquad (35)$$

$$p^* = 0 \ . \qquad (36)$$

In the crab mode, the control law crabs the aircraft into the wind while maintaining null aiming errors. Substituting Eq (30) and Eq (34) in Eqs (4) (8) (11) gives the desired values

$$r^* = -\left(1 - \frac{V}{V+V_m}\right)\frac{v_w}{V\tau} \qquad (37)$$

for yaw rate, and

$$p^* = -r^* \tan\theta^* \qquad (38)$$

for roll rate. Thus, in the crab mode, the aircraft must change heading continuously to keep the sightmark lined up on the target ; the yaw rate which is dependent on the crosswind magnitude increases as range decreases.

If DSF is not available, the desired path is defined as a 9th order system in 10 unknowns. In this case, crosswind can be trimmed by commanding the aircraft to roll in the appropriate side, the amount of bank angle required being dependent only on the crosswind magnitude in the decrabbed flight mode, on both crosswind magnitude and range in the crabbed flight mode.

For crosswinds of small magnitude (under 10 m/s), it is appropriate to compute the desired flight path by using a model of aircraft dynamics in which the longitudinal motion and the lateral motion are decoupled.

Remark : Under zero crosswind, an alignment manoeuvre similar to the crab mode can be achieved by selecting a desired flight path where the sideslip is not null ($v^* = v_d$) and the corresponding desired values of yaw rate and roll rate are given by :

$$r^* = \left(1 - \frac{V}{V+V_m}\right)\frac{v_d}{V\tau}$$

$$p^* = -r^* \tan\theta^* \ .$$

In an hostile environment, such a manoeuvre can increase aircraft survivability.

Implementation : A schematic diagram of the IFFC system is shown in Figure 7.

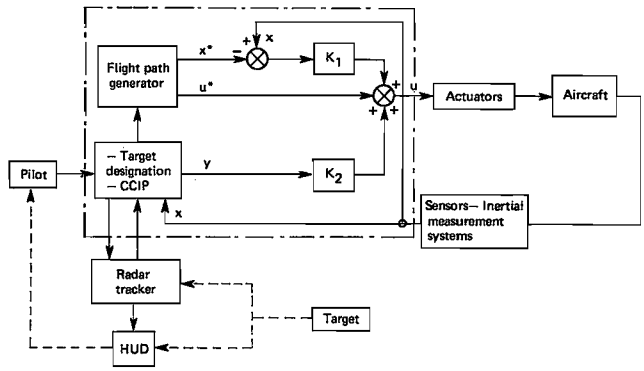

Fig. 7 – IFFC air-to-ground gunnery schematic.

One can imagine IFFC system operation with associated implementation described as follows : the pilot takes control of the radar by pushing a button on the side of the throttle. The same button then serves to move a cursor on the HUD. After designation, the radar locks automatically on the target ; target range is fed to the fire control computer ; target position, bullet impact point are then displayed on the HUD. After engagement, the IFFC system nulls aim error automatically and maintains the aircraft path as close as possible to the desired path so that weapon can be released at any range. Using the designation button, the pilot may slew the cursor to achieve better lock-on or to change target during the pass.

IV.2. Results from digital simulation

The performance of the IFFC system described above has been evaluated using the same nonlinear digital simulation of a typical combat aircraft as in Section III. The initial conditions of the gunnery pass are described in Section II. Thus, after designation of the target, the IFFC system is engaged at a range of 2,500 m to null aiming errors. Feedback gains are only dependent on target range, numerical values corresponding to the beginning and end of the pass are given in Appendix 2.

Responses to initial longitudinal offset (see Fig. 8) show that aiming error Σ_w is nulled within 2 seconds with a slight overshoot ; the desired path is reached within the same time interval. Because firing ranges seldom exceed 2,000 m, it has been found appropriate, in the IFFC system, to use fictitious ballistic corrections corresponding to a 2,000 metre-fixed firing range whenever the actual aircraft-to-target distance was over 2,000 m, thus avoiding nulling excessive aiming errors when the aircraft is too distant from the target. When reaching 2,000 metres, the use of correct ballistic corrections in the IFFC system causes a slight change in the desired flight path which produces incidental effects on the elevator deflexion.

Responses to initial lateral offset are shown in Fig. 9. Lateral aiming error Σ_v has a larger time of response than Σ_w ; the associated transient sideslip has a peak value of about 0.6 deg. per degree of Σ_v . However, the use of DSF during a similar manoeuvre has great impact on lateral aiming performance as can be seen from Fig. 9 : transient values of sideslip and roll rate are smaller and aim error response is achieved in a shorter time. Indeed, in a conventional aircraft (without DSF), the time required to bank the aircraft introduces a significant time lag in the heading change manoeuvre.

Both decrab and crab control laws are effective in nulling lateral aiming errors in presence of a significant crosswind. The results obtained with a typical lateral wind profile are presented in Figs. 10 and 11. In the decrab mode, the acceleration generated by the DSF control surfaces saturates at 1 g during 0.5 sec. and the roll angle required to turn the aircraft in the transient phase is more important than in the crab mode. Projections on an horizontal plane of the aircraft flight paths obtained with both alignment manoeuvre modes are compared in Fig. 12 ; in the decrab mode the aircraft body axis is aligned with the ground track once the desired path has been reached, while in the crab mode the aircraft changes heading continuously with a yaw rate increasing as range to target decreases. In both cases, weapon can be released at any range, 3 seconds after IFFC engagement.

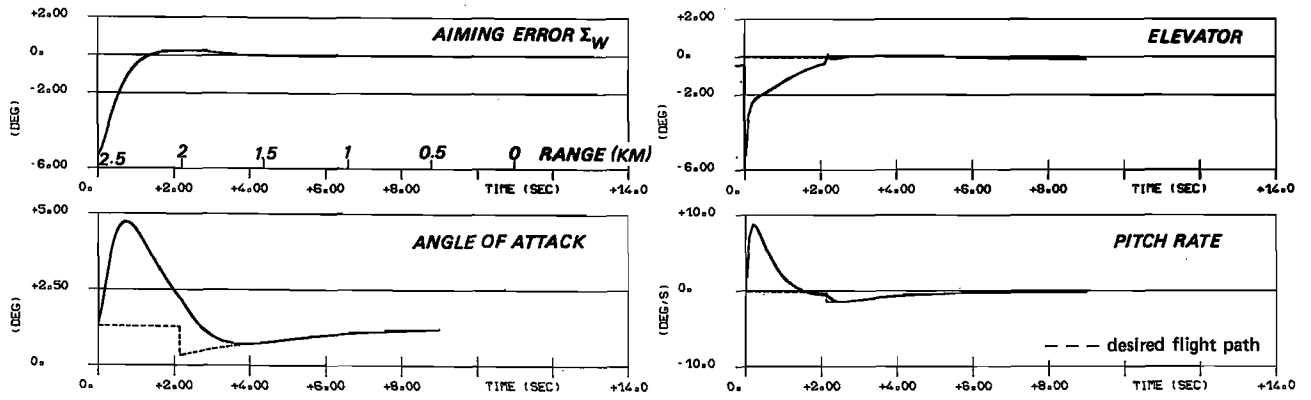

Fig. 8 — Longitudinal aiming response.

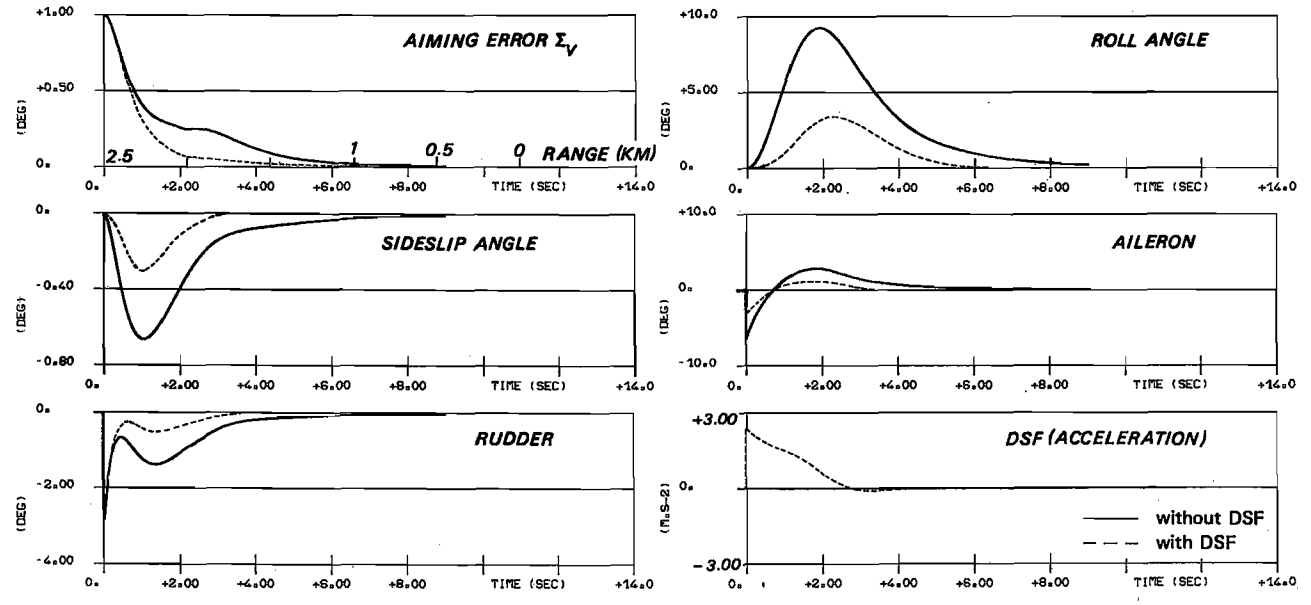

Fig. 9 — Lateral aiming response (crosswind = 0).

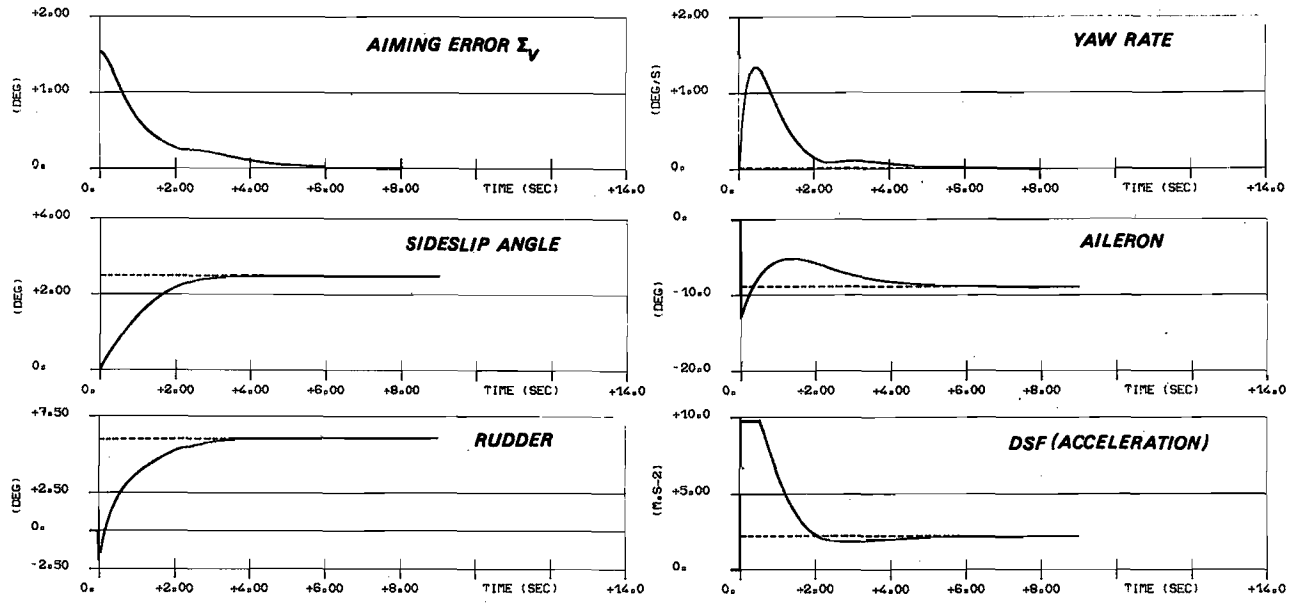

Fig. 10 — Lateral aiming response in the decrab mode. (see fig. 12 for the crosswind profile).

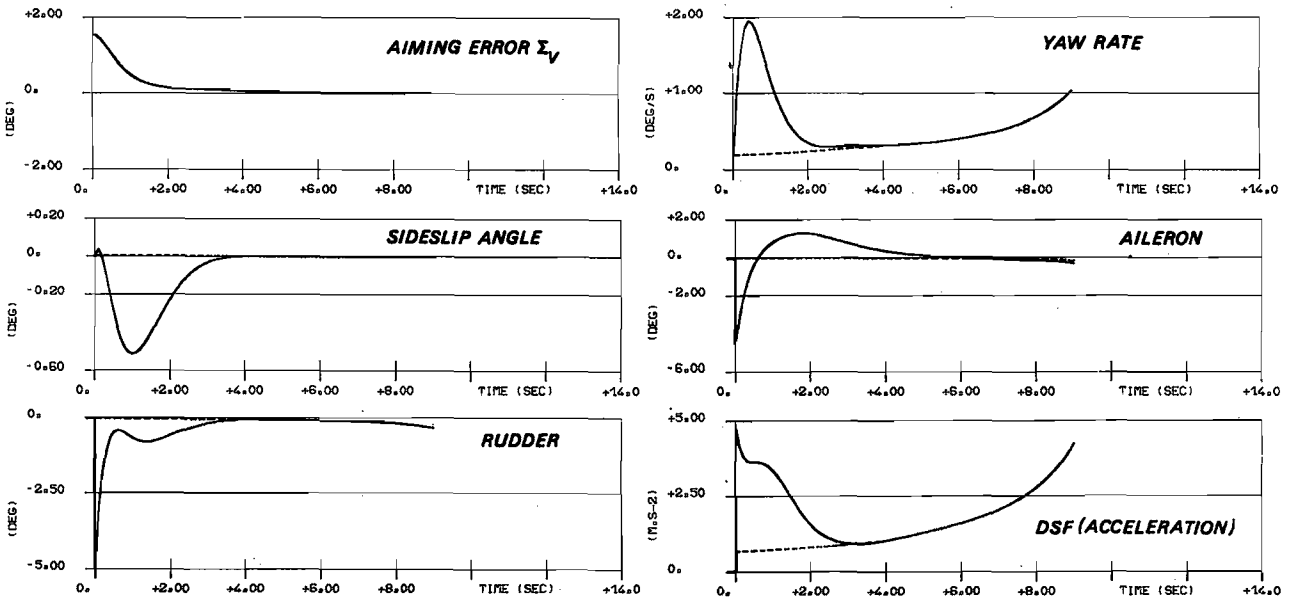

Fig. 11 — Lateral aiming response in the crab mode. (see fig. 12 for the crosswind profile).

IFFC gunnery display shown in Fig. 13 depicts what the pilot see in the HUD during the pass. The mean wind profile is the same as used in the previous simulations. Although longitudinal-lateral coupling in the aircraft motion has been neglected in computing the feedback gains, the established linear control law still gives satisfactory results in aiming accuracy ; the aiming error is indeed reduced to 0.2 deg. only 2 seconds after IFFC engagement, the IFFC system then holds the sightmark on the target throughout the pass with a precision of 0.1 deg., till the pilot commands the evasive manoeuvre. Inclusion of the coupling mentioned above will be justified whether the improvement in accuracy is enough significant.

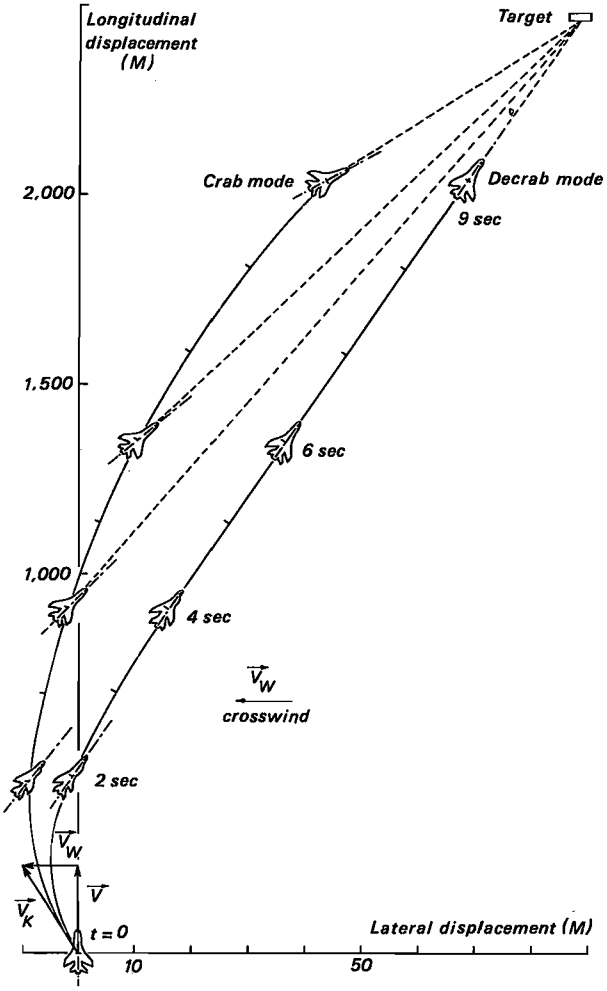

V. Conclusion

This paper has presented a new concept of aircraft control based on manoeuvre commands in opposition to control surface deflexion commands. Improved handling qualities of aircraft, reduced pilot's workload are the principal goals in the use of such a system.

A sideslip-roll rate-pitch rate command system has been tested to evaluate gun pointing effectiveness in air-to-ground gunnery. From digital simulation results, it appears that pitch rate command is well adapted to null longitudinal offset but yaw rate command should be preferred to roll rate command to null lateral offset.

In order to reduce further the pilot's workload and to improve further weapon accuracy, an Integrated Flight and Fire Control (IFFC) system has been studied and evaluated for a typical combat aircraft in air-to-ground gunnery. In the design presented here, the pilot input is reduced to target designation and the commands to the flight control system are generated by errors between computed bullet impact point and target position. Once aiming errors are nulled, the IFFC system manoeuvres the aircraft to follow a desired flight path along which ballistic corrections are taken into account so that weapon can be released at any range. Both crab mode and decrab mode are effective for alignment in presence of crosswinds.

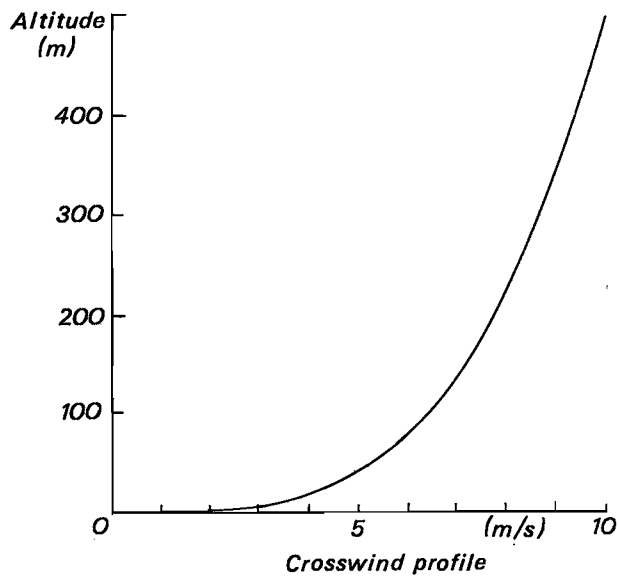

Fig. 12 – Decrab and crab mode alignment manoeuvres.

Fig. 13 – Target and bullet impact point trajectories in HUD during gunnery pass (crab mode).

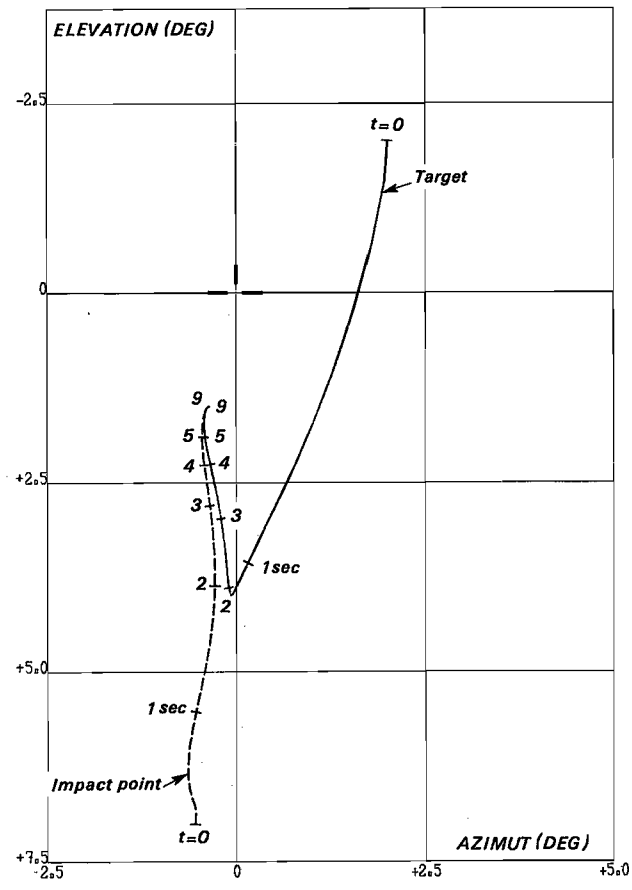

References

1 Quinlivan, R.P., The need for task-oriented control laws, AGARD Lecture No 4, 89 th AGARD-LS on "Task-Oriented Flight Control Systems", June 1977.

2 Kirszenblat, A., Calcul d'un système de commande à deux niveaux du mouvement non linéaire d'un avion, NT ONERA No 1979-7, 1979.

3 Huber, R.R., Integration of flight and fire control, AGARD Paper No 65, 272nd AGARD-CP on "Advances in Guidance and Control Systems using Digital Techniques", May 1979.

4 Cdt Sourdon, Tir aérien théorique, Section d'Instruction et d'Etude du Tir, B.A. 120 Cazaux, 1978.

5 Balança, J., Utilisation de la force directe latérale. Application au tir air-sol, unpublished ONERA report, 1980.

6 Athans, M. and Falb, P.L., Optimal control, Mc Graw Hill, N.Y., 1966.

7 Kreindler, E. and Rothschild, D., Model following in linear quadratic optimization, AIAA Journal Vol. 4 No 7, July 1976.

8 Kwakernaak, H. and Sivan, R., Linear optimal control system, J. Wiley & Sons, N.Y., 1972.

Appendix 1

Equations of aircraft motion (in a principal inertial reference frame)

$$\dot{v} = Y_v v + Y_p p + Y_r r + Y_{\delta_\ell}\delta_\ell + Y_{\delta_n}\delta_n + Y_{\delta_{DSF}}\delta_{DSF} - rV + pw + g\cos\theta\sin\phi - \dot{v}_w + pw_w$$

$$\dot{w} = Z_o + Z_w w + Z_q q + Z_{\delta_m}\delta_m + qV - pv + g\cos\theta\cos\phi - \dot{w}_w - pv_w$$

$$\dot{p} = L_v v + L_p p + L_r r + L_{\delta_\ell}\delta_\ell + L_{\delta_n}\delta_n + L_{\delta_{DSF}}\delta_{DSF} + \frac{I_y - I_z}{I_x} qr$$

$$\dot{q} = M_o + M_w w + M_q q + M_{\delta_m}\delta_m + \frac{I_z - I_x}{I_y} pr$$

$$\dot{r} = N_v v + N_p p + N_r r + N_{\delta_\ell}\delta_\ell + N_{\delta_n}\delta_n + N_{\delta_{DSF}}\delta_{DSF} + \frac{I_x - I_y}{I_z} pq$$

$$\dot{\phi} = p + (q\sin\phi + r\cos\phi)\tan\theta$$

$$\dot{\theta} = q\cos\phi - r\sin\phi$$

Appendix 2

Aircraft data (angles and control deflexions in radians)

$I_x = 6,500\ kgm^2$ $I_y = 82,500\ kgm^2$ $I_z = 88,000\ kgm^2$

$V = 230\ m/s$

$Y_v = -0.35$ $L_v = -0.16$ $N_v = 0.02$ $Z_o = -3.15$ $M_o = 0.13$

$Y_p = 0$ $L_p = -1.86$ $N_p = -0.05$ $Z_w = -1.15$ $M_w = -0.04$

$Y_r = 0$ $L_r = 0.40$ $N_r = -0.28$ $Z_q = 0$ $M_q = -2.28$

$Y_{\delta_\ell} = 0$ $L_{\delta_\ell} = -6.05$ $N_{\delta_\ell} = -0.29$ $Z_{\delta_m} = -28.8$ $M_{\delta_m} = -29.3$

$Y_{\delta_n} = 11.9$ $L_{\delta_n} = 6.16$ $N_{\delta_n} = -2.24$

$Y_{\delta_{DSF}} = 10$ $L_{\delta_{DSF}} = 0$ $N_{\delta_{DSF}} = 0$

Feedback gain matrices (units : metre, second, radian)

(v, p, q) command system :

$$K_P = \begin{bmatrix} 0.06 & 0 & 0.96 & 0 & 0.22 \\ 0 & -0.01 & 0 & 0.71 & 0 \\ 0.03 & 0 & -0.08 & 0 & 2.01 \end{bmatrix} \quad K_I = \begin{bmatrix} 0.002 & 4.75 & 0 \\ 0 & 0 & 0.08 \\ -0.01 & -0.42 & 0 \end{bmatrix}$$

IFFC system :

$$K_1 = \left[\begin{array}{c|c|c|c|c|c|c} -0.001 & 0 & 0.09 & 0 & 1.35 & 0.27 & 0 \\ 0 & -0.001 & 0 & 0.48 & 0 & 0 & 0 \\ 0.006 & 0 & -0.05 & 0 & 1.81 & 0.005 & 0 \\ -0.08 & 0 & 0.14 & 0 & -2.70 & -0.48 & 0 \end{array}\right] \quad K_2 = \begin{bmatrix} -2.76 & 0 \\ 0 & 1.06 \\ -2.99 & 0 \\ 14.7 & 0 \end{bmatrix}$$

for range $= 2,500m$ $(t_o = 0)$

$$K_1 = \left[\begin{array}{c|c|c|c|c|c|c} 0.003 & 0 & 0.10 & 0 & 1.38 & 0.31 & 0 \\ 0 & -0.003 & 0 & 0.48 & 0 & 0 & 0 \\ 0.01 & 0 & -0.05 & 0 & 1.80 & 0.01 & 0 \\ -0.14 & 0 & 0.16 & 0 & -4.46 & -0.88 & 0 \end{array}\right] \quad K_2 = \begin{bmatrix} -4.14 & 0 \\ 0 & 1.39 \\ -3.83 & 0 \\ 30.8 & 0 \end{bmatrix}$$

for range $= 500m$ $(t_f = 9\ s)$

Model of desirable aim error kinematics :

$$A_m = \begin{bmatrix} -2 & 0 \\ 0 & -2 \end{bmatrix}$$